Chapter 11

Transmission Electron Microscopy of Platelets FROM Apheresis and Buffy-Coat-Derived Platelet Concentrates

Josef Neumüller, Adolf Ellinger and Thomas Wagner

Additional information is available at the end of the chapter

http://dx.doi.org/10.5772/60673

Abstract

Platelet concentrates are produced in order to treat bleeding disorders. They can be provided by apheresis machines or by pooling of buffy coats from four blood donations. During their manufacturing and storage, morphological alterations of platelets occur which can be demonstrated by transmission electron microscopy. Alterations range from slight and reversible changes, such as formation of small cell protrusions and swelling of the surface-connected open canalicular system, to severe structural changes, where platelets undergo transitions from discoid to ameboid shapes as a consequence of platelet activation. These alterations end in delivery of the contents of platelet granules as well as platelet involution caused by apoptosis and necrosis processes denoted as the platelet release reaction. Hereby, the involvement of the network of the open canalicular system, helping to deliver the contents of platelet granules into the surrounding milieu via pores, is distinctly shown by electron tomography. As a consequence of platelet activation, a delivery of differently sized microparticles takes place which is thought to play an important role in the adverse reactions in some recipients of platelet concentrates. In this article, the formation and delivery of platelet microparticles is illustrated by electron tomography. Above all, the ultrastructural features of platelets and megakaryocytes are discussed in the context of the molecular characteristics of the plasma membrane and organelles including the different granules and the expression of receptors engaged in signaling during platelet activation. Starting from the knowledge of the ultrastructure of resting and activated platelets, a score classification is presented, allowing the evaluation of different activation stages in a reproducible manner. Examples of evaluations of platelet concentrates using electron microscopy are briefly reviewed. In the last part,

experiments showing the interaction of platelets with bacteria are presented. Using the tracer ruthenium red, for staining of the plasma membrane and the open canalicular system of platelets as well as the bacterial wall, the ability of platelets to adhere and sequestrate bacteria by formation of small aggregates, but also to incorporate them into compartments of the open canalicular system which are separated from the surrounding milieu, was shown. In conclusion, electron microscopy is an appropriate tool for the investigation of the quality of platelet concentrates. It can efficiently support results on the functional state of platelets obtained by other methods such as flow cytometry and aggregometry.

Keywords: Platelet concentrates, Quality control, Platelet ultrastructure, Platelet activation, Platelet microparticles, Uptake of bacteria

1. Introduction

Platelet concentrates (PCs) are indispensable biopharmaceuticals for treatment of bleeding disorders. Indications for PC transfusions are either prophylactic, to prevent hemorrhage in oncohematology, or therapeutic, using limited platelet (PLT) transfusion to actual bleeding episodes. They are also applied to treat hematologic patients undergoing surgery and invasive procedures and disorders of PLT function, such as Glanzmann's thrombasthenia, Bernard–Soulier syndrome, Gray and White platelet syndrome, Storage Pool disease, Scott syndrome, and Disseminated Intravascular Coagulation [1]. Above all, massive PLT transfusions are indicated for treatment of Refractory Autoimmune Thrombocytopenias [2]. The short storage period of five days, where PC can be used for transfusion, reflects the high sensitivity of these cell fragments. This sensitivity is related to the high reactivity of PLTs in respect to their activation potential but also to their fragility. PCs can be produced by a variety of manufacturing processes which affect more or less the viability and reactivity of PLTs. Several publications report on this subject [3–15].

The reactivity of PLTs in the recipient of a PC can only be estimated through the recovery of the hemostatic balance. To date, no function test is adequate to reliably predict PLT behavior in vivo following transfusion [16]. A few laboratory tests available provide insufficient or conflicting results [17]. Therefore, it is obligatory in blood banking to determine the quality of the PC itself. Nevertheless, it can be assumed that irreversible PLT activation during processing would impair PLT functionality in vivo. It has been shown that activated PLTs stored for 3 days can provoke activation of T cells, B cells, and monocytes of the recipient [18]. During storage of PC, activation and release of inflammatory mediators may occur, leading to adverse effects in transfused patients after cardiac surgery [19]. Above all, the formation of platelet membrane microparticles (PMPs) contributes to the induction of adverse transfusion reactions by facilitating cell–cell interactions with cells of the recipient including signal transduction and even receptor transfer [20]. PMPs could also play a role in anaphylactic transfusion reactions [21].

http://dx.doi.org/10.5772/60673

Electron microscopy has been used to investigate the complex and highly dynamic structure of the PLT cytoplasm, including their specific organelles that are primarily formed in the megakaryocyte (MK) from which they originate.

The ultrastructure of platelets and MKs as well as highlights of their discovery are presented in Chapter 1 in the form of a historical overview. In Chapter 2, we describe the ultrastructure of MKs, PLTs in resting and activated forms, as well as PMPs using conventional fixation methods and advanced methods such as high-pressure fixation, cryosectioning, and cryosubstitution representing state-of-the-art EM techniques. In Chapter 3, we discuss where EM can efficiently support commonly used routine methods for quality assessment of PCs such as the flow cytometry and light microscopic methods or aggregometry in respect to the viability and activation of their particular PLT. In Chapter 4, results on the interaction of bacteria with platelets are presented. We discuss whether PLT are able to phagocytize bacteria or only sequestrate them by uptake into the surface-connected open canalicular system or by the formation of aggregates.

2. Ultrastructure of platelets and megakaryocytes

2.1. Historical overview

Most of the EM reports about PLT were published in the last four decades of the twentieth century starting from the early 1970s. A remarkable number of reports were published by James G. White (University of Minnesota, Minneapolis, USA), who focused in his oeuvre on the ultrastructural investigation of platelets in healthy condition [22–40] but also in several PLT-associated disorders [41–49]. Marcel Bessis (Centre Nationale de Transfusion Sanguine, Paris, France) was one of the first who investigated megakaryocytes and PLT among other blood cells ultrastructurally [50, 51]. In the following years, fine structural features of PLT have been described, such as the microtubular coil (MTC) providing the discoid shape of non-activated PLT [40, 52–60], the microfilamentous network providing their contractile apparatus [29, 53, 55, 61, 62], and the surface-connected open canalicular system (OCS). The latter represents an invagination of the plasma membrane providing a connection with the outer milieu via pores at the surface and a two-way channel for uptake of particles and the delivery of granular contents during activation and degranulation [24, 34, 35, 63–65]. Furthermore, the dense tubular system (DTS), originating from the endoplasmic reticulum of MKs [66–76] and small Golgi systems [47, 77–80], has been described. Three types of PLT granules have been identified morphologically and by histochemical and immunohistochemical methods: dense granules [22, 80], α-granules [28, 30, 58, 82–85], and lysosomes [72, 78]. Immunogold labeling allowed the identification of PLT receptors at the plasma membrane and along the invaginations of the OCS. In this way, Stenberg et al. identified the CD62P receptor (GMP-140) in unstimulated and in thrombin-activated PLTs [79]. Lewis et al. [80] showed contact sites leading to aggregated PLTs involving fibrinogen and its receptor GPIIb/IIIa via immunogold labeling of whole-mount PLT preparations and high-voltage transmission electron microscopy. In these preparations, granulomeres could be easily distinguished from hyalomeres, separated by a filamentous network. GPIIb/IIIa-positive regions could be identified at cell contacts, in the surroundings of the granulomere, as well as inside the OCS.

2.2. Megakaryocytes and the formation of platelets

For understanding the fine structural features in the function of PLTs, dynamic processes with respect to the rearrangement of organelles, above all of the membranous components, are important (Figure 1).

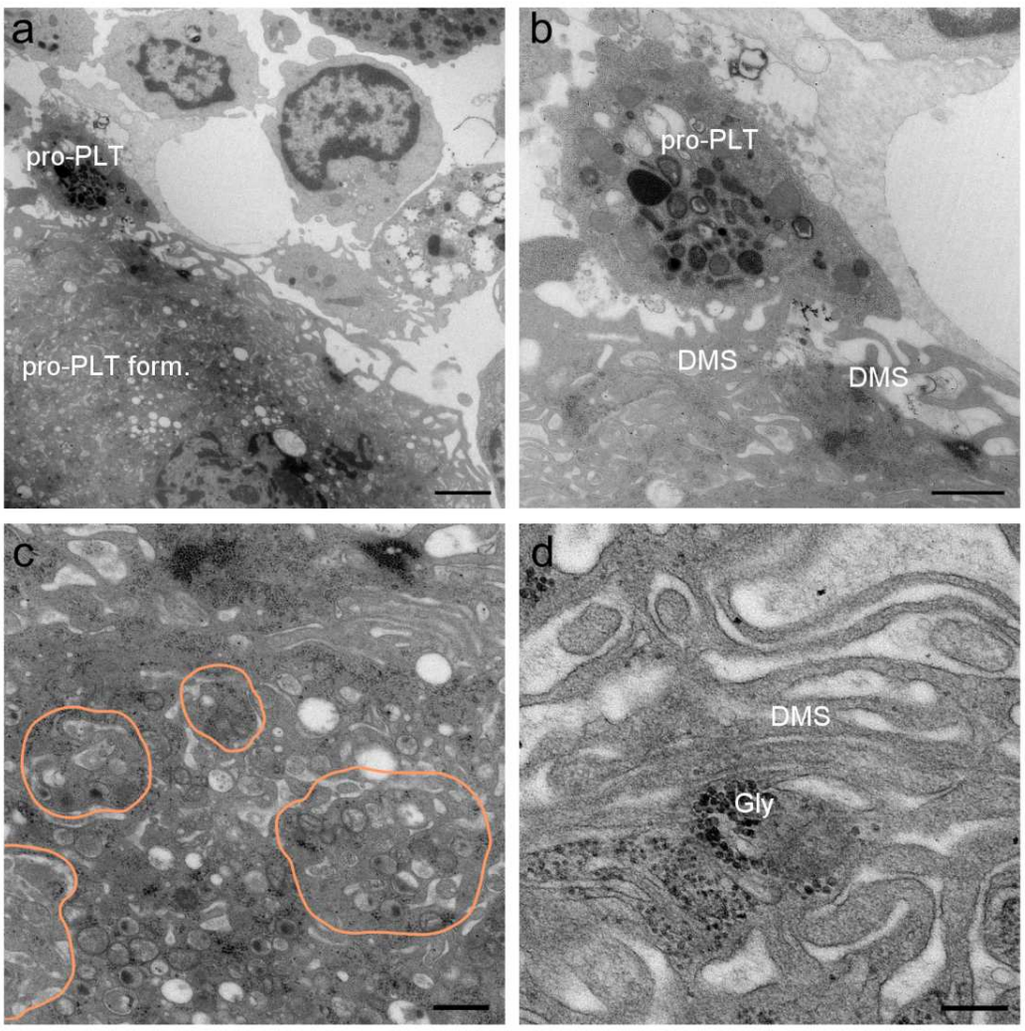

Figure 1. Aspects of an MK. In Figure 1a, the delivery of a pro-PLT is shown. The region where pro-PLT (pro-PLT form) surrounded by the DMS are formed is visible. Note the huge lobulated nucleus (N). Figure 1b: Same aspect at higher magnification. The delivered pro-PLT is still connected with a network, formed by the DMS. Figure 1c: The assembly of organelles of newly formed pro-PLTs is indicated by colored contours. Figure 1d: Pleomorphous regions of the DMS surrounding granules and glycogen aggregates (Gly). Size bars: 2 μm in Figure 1a, 1 μm in Figure 1b, 500 nm in Figure 1c,d. The samples were routinely prepared by chemical fixation, dehydration, and embedding in Epon, and 70 nm ultrathin sections were viewed under a Tecnai 20 (FEI Co.) at 80 KV acceleration voltage. Digital images were acquired using an Eagle 4k bottom-mount camera (FEI Co.).

Recently, Machlus and Italiano Jr. reviewed the development of PLTs, starting from MK development to PLT formation [81]. MKs are the rarest but also the largest cells (50–100 μm in diameter) of the bone marrow. They mature at the hematopoietic niche (osteoblastic niche) and travel to the bone marrow sinusoids (vascular niche) in order to deliver 10–20 pro-PLTs

http://dx.doi.org/10.5772/60673

into the bloodstream. The maturation process, starting from hematopoietic stem cells, is driven by thrombopoietin which binds to the MK-specific receptor MP-1 [82–84]. Under the influence of thrombopoietin, the nuclei of MKs enlarge by endomitosis, increasing their DNA content of 4n, 8n, 16n, 32n, 64n, and even 128n. Obviously, the reason for the augmentation of DNA in a single nucleus is to provide a sufficient amount of m-RNA in order to form the equipment for newly formed pro-PLTs while maintaining full functionality of the whole cell [85]. Between the lobules of the polyploid nucleus, the DMS is formed from the plasma membrane. Required membranes are provided by the Golgi apparatus via the trans-Golgi network but also by the endoplasmic reticulum [86]. Using laser confocal microscopy, electron tomography, and focused ion beam scanning electron microscopy, these authors could show that at all developmental stages of MKs, the DMS was in continuity with the PM and that the number of these connections correlated with nuclear lobulation. They propose that at early MK development stages, a PM invagination process takes place that resembles cleavage furrow formation. During MK maturation, the DMS enlarges to a conspicuous network of tubules and cisternae distributed throughout the whole cytoplasm. The DMS needs support from the cytoskeleton provided mainly by spectrin; it is essential for the formation of the PM of pro-PLTs [87].

In the terminal maturation process of MKs, long cell extensions, composed of pro-PLTs, extend into the sinusoidal vessels of the bone marrow, a process also guided by the cytoskeleton. The pro-PLT elongation is provided mainly by β1-tubulin [88]. In a later publication, this author described also a new stage of PLT formation; the pre-PLT which can convert into a barbell-like pro-PLT form, subsequently dividing into two newly formed PLTs [89].

The question how pro-PLTs can pass the wall of the bone marrow sinusoids has been elucidated by the detection of podosomes which represent micrometer-sized, highly dynamic circular protrusions of the PM of MK and other cells such as osteoclasts, macrophages, dendritic cells, and endothelial cells [90, 91]. Podosomes are adhesion domains consisting of F-actin-rich cores with integrin-associated ring structures. Typical core proteins include Arp2/3 complex, WASp, and cortactin, whereas integrins, vinculin, talin, paxillin, and myosin IIA localize to the ring structure [92]. The authors could also demonstrate that MK podosomes are able to degrade extracellular matrix using matrix metalloproteinases. EM contributed significantly to visualization and understanding of podosomes. Former publications demonstrated the actin filament arrangement in core and network [93, 94]. In more recent works, podosomes have been investigated in 3D environments [95–98] using super-resolution light microscopic techniques such as STED (stimulated emission depletion), dSTORM (direct stochastic optical reconstruction microscopy), and PALM (photoactivated localization microscopy) that complement electron microscopic capabilities.

2.3. The ultrastructure of platelets

PLTs are the smallest cellular blood components (Figure 2). They are discoid cell fragments with a remarkable equipment of dynamic organelles but lacking a nucleus. Their diameter varies between 2 and 3 μm, but their thickness is only less than 1 μm. In human peripheral blood, the absolute number of PLT ranges from 150,000 to 450,000 per ml. The average lifetime in the circulation is 5 to 11 days. After this time, they become degraded in the spleen but also in the liver and in the lung.

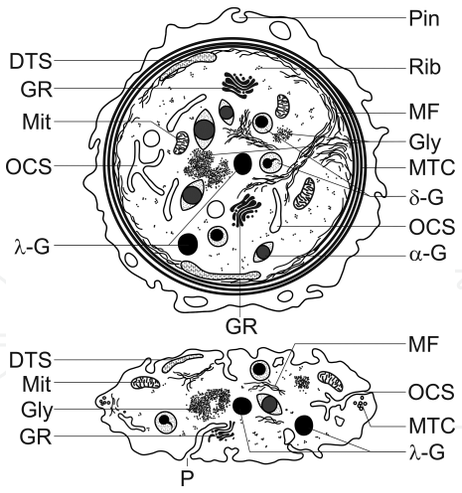

Figure 2. A scheme of a PLT in the equatorial plane (upper image) and in cross section (image at the bottom). Abbreviations: DTS *dense tubular system*, Gly *glycogen*, α *α-granules*, δ *δ-granules or dense bodies*, λ *λ-granules or lysosomes*, GR *Golgi remnants*, MF *microfilaments*, Mit *Mitochondria*, OCS *open canalicular system*, P *pores of the OCS*, Rib *ribosomes*.

PLTs circulate under normal health conditions in a quiescent discoid stage that is maintained by the anti-homeostatic properties of the endothelium that lines the inner wall of the entire vasculature. After vessels are injured due to trauma or pathological conditions such as atherosclerosis and diabetes, where a degeneration of endothelium takes place, PLTs become activated and change their shape dramatically acquiring an ameboid form due to the rearrangement of organelles, triggered by microtubules and microfilaments.

An ongoing activation takes place if PLTs adhere to a glass surface. After a few minutes, a characteristic compartmentalization in a dense central granulomere and a peripheral lucent hyalomere can be seen already under the light microscope (Figure 3).

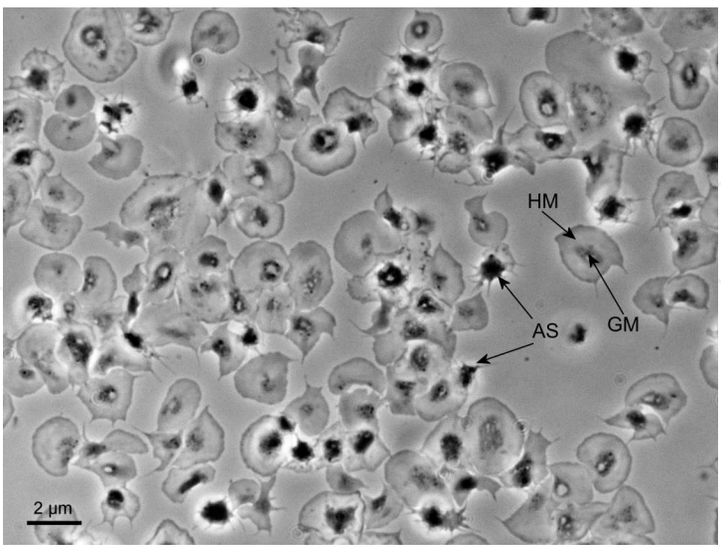

Figure 3. Light microscopic picture of glass-adherent PLTs, incubated for 15 min in phosphate buffered saline. Hyalomere (HM) and granulomere (GM) are clearly visible. Some adherent PLTs show an ameboid shape (AS) as a sign of activation.

http://dx.doi.org/10.5772/60673

In TEM, the granulomere is surrounded by a contractile ring of cytoskeleton elements. The granulomere contains not only different species of granules but also parts of the surface-connected OCS, mitochondria, and glycogen. Parts of the DTS line the marginal cytoskeletal ring (Figure 4b). Resting discoid PLTs contain a peripheral stabilizing microtubular ring built up of β-tubulin (Figure 4a). This ring represents a circumferential MTC consisting of one microtubule wound 8–12 times stabilizing the PLT shape. During PLT activation, the MTC is primary contracted and then fragmented and dislocated to the newly formed filopodia.

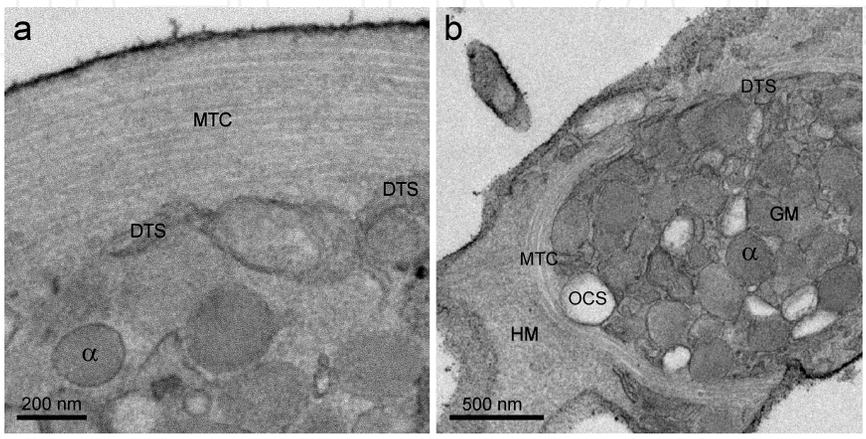

Figure 4. TEM of glass-adherent PLTs, fixed for 5 min (a) and 15 min (b) after incubation. Figure 4a shows the MTC and in close vicinity the DTS. In Figure 4b, hyalomere and granulomere appear separated by the MTC and can be clearly distinguished. Abbreviations as in Figure 2.

The DTS triggers the resting stage as well as the transition into the activation process of PLTs. It originates from the rough endoplasmic reticulum of MK. It has an irregular form, and in resting PLTs, it is located close to the MTC. Its peroxidase content allows to contrast it via a diaminobenzidine reaction. In contrast to the OCS, it contains slightly electron-dense amorphous material. Lipid-modifying enzymes such as cyclooxygenase and thromboxane synthetase catalyze downstream metabolites of the arachidonic acid degradation pathway and the delivery of thromboxane into the extracellular milieu. The PLT activation is regulated by the maintenance of calcium storage which is controlled by the action of a membrane-associated pump (sarcoplasmic reticulum Ca^{2+} ATPase) and by the action of the second messenger cAMP that initiates the delivery of Ca^{++} into the cytosol inducing PLT activation.

As mentioned above, PLTs are interlaminated by the OCS originating from the DMS of MKs and are connected as well with the outer milieu via pores (Figure 5).

The cytoplasm contains α-, δ-, and λ-granules and the dense tubular system which derives from the endoplasmic reticulum of MKs. Ribosomes and polyribosomes as well as few mitochondria are also present as equipment remaining from MKs. PLTs also contain often a high number of accumulated glycogen granules.

alpha-granules contain proteoglycans, hemostasis factors and cofactors (fibrinogen, factors V, VII, XI, and XIII, kininogens, protein S, and plasminogen), adhesive matrix proteins (fibronectin (FN), vitronectin (VN), thrombospondin (TSP), von Willebrand factor (vWF), adhesion

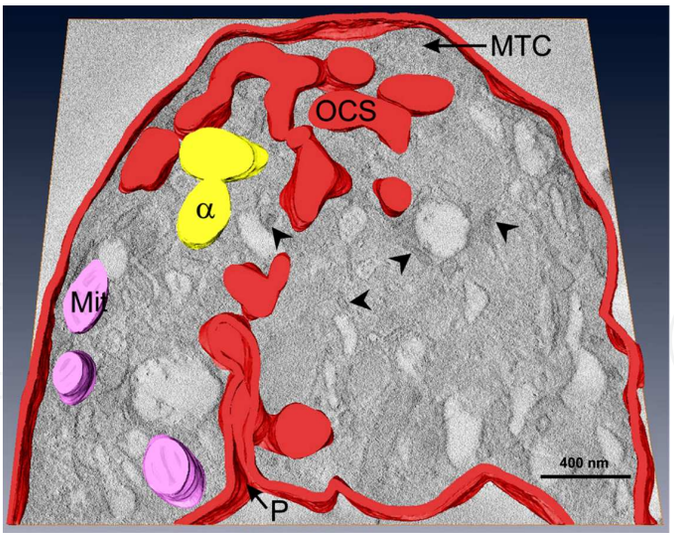

Figure 5. Electron tomographic 3D model of the OCS showing a pore (P) connecting it with the surrounding milieu. The DTS is indicated by arrowheads. One virtual slice is shown in background. The electron tomographic acquisition was performed on a Tecnai 20 (FEI Co., Eindhoven, The Netherlands). Using 200 nm semithin sections, tilt series were started from –65 ° to +65 ° with 1 ° increment by the help of the Xplore3D software (FEI Co.). Reconstruction of the tilt series was performed with the IMOD software (Boulder Laboratories, University of Colorado). The model was drawn using the Amira 4.1 software (Mercury Computer Systems, Merignac, Cedex, France). For abbreviations, see Figure 2.

molecules such as GP140 (CD62P), cytokines and chemokines like RANTES and interleukin 8, as well as several growth factors: TGF-β (transforming growth factor-β), PDGF (platelet-derived growth factor), ECGF (platelet-derived endothelial growth factor), VEGF (vascular endothelial growth factor), bFGF (basic fibroblast growth factor), EGF (epidermal growth factor), and IGF (insulin-like growth factor). In addition, protease inhibitors, albumin and immunoglobulins are stored in α-granules.

Dense granules (δ-granules) are the smallest ones with a diameter of about 150 nm. Their name is related to their strongly electron-dense core, surrounded by a clear space enclosed by a single membrane. These organelles develop in early MKs where they look primarily empty, acquiring their dense core by incorporation of adenine nucleotides and serotonin during maturation. They contain a metabolic inert adenine nucleotide pool and store serotonin at concentrations of about 65 mM. In addition, they contain a high amount of bivalent cations—predominantly calcium—that is not mobilized in the course of PLT activation.

Lysosomes (λ-granules) exhibit a lower electron density than δ-granules. They contain lysosomal enzymes playing a role in clot formation but also in antibacterial defense such as acid proteases and glycoproteases. The lysosomal membrane contains the integral membrane protein LIMP (CD63) which is transferred to the plasma membrane during PLT activation as well as the two membrane-associated glycoproteins LAMP-1 and LAMP-2. CD63 is used as a PLT activation marker and can be routinely demonstrated by flow cytometry using fluorola-beled monoclonal antibodies.

The ultrastructure of PLTs as well as the release reaction of granule contents during PLT activation has been summarized in an excellent review [72].

http://dx.doi.org/10.5772/60673

In the past two decades, new methodical and technical developments, such as cryofixation combined with freeze substitution, were applied for the investigation of PLT morphology, avoiding the problems of chemical fixation-dependent artifacts. In addition, the implementation of electron tomography allowed a better understanding of the three-dimensional architecture of PLT organelles. In this respect, many views about cytoskeleton and the internal structure of granules had to be revised [99]. It could be impressively demonstrated that the OCS and the DTS are highly intertwined, forming close associations in specialized membrane regions. These authors discerned three subtypes of α-granules based on morphological features: first, spherical granules with an electron-dense and electron-lucent zone containing microtubules built up of vWF multimerin elements and a diameter of 12 nm; a second type containing a multitude of luminal vesicles, 50 nm wide tubular organelles; and a third population with 18.4 nm crystalline cross striations. Using electron tomography, the authors could impressively reveal the spatial arrangement of these organelles.

The plasma membrane is the site where a multitude of receptors is present that can interact with soluble ligands, with cellular counter receptors on other PLTs, on leucocytes, or on endothelial cells, with molecules of the extracellular matrix but also with pathogens. These receptors play an important role in inside–outside signaling in the course of PLT activation and the release reaction. As outlined in a review by Rivera et al. in 2009 [100], many types of mobile transmembrane receptors are present at the PLT membrane, including many integrins (αIIbβ3, α2β1, α5β1, α6β1, αVβ3), leucine-rich repeat (LRR) receptors (glycoprotein [GP] Ib/IX/V, toll-like receptors), G-protein coupled seven-transmembrane receptors (GPCR) (PAR-1 and PAR-4, thrombin receptors, P2Y1 and P2Y12 ADP receptors, TPα and TPβ (TxA2 receptors), proteins belonging to the immunoglobulin superfamily (GP VI, FcγRIIA), C-type lectin receptors (P-selectin), tyrosine kinase receptors (thrombopoietin receptor, Gas-6, ephrins, and Eph kinases), and a miscellaneous of other types (CD63, CD36, P-selectin glycoprotein ligand 1, TNF receptor type, etc.). Many of these receptors have been characterized using immune electron microscopy [30, 33, 73, 74, 79, 80].

New methods have been developed allowing to share the results from biochemistry, laser confocal microscopy, and EM to explain the different steps in PLT activation starting from Ca^{++} mobilization of the dense tubular system, the degranulation process of dense granules followed by the delivery of the contents of α-granules and lysosomes via docking and fusion of the membranes of granules with the membrane of the OCS using the SNARE machinery [101].

2.4. Platelet activation and the release reaction

By EM, PLT changes and signs of activation due to preparatory influences can precisely be determined and classified. Canizares and coworkers [61] showed the different steps of PLT activation in detail. Their classifications include six stages: (1) the unaltered discoid form; (2) the pseudotubular form (very slight activation) when the peripheral MTC disappears, a pseudotubular membranous structure occurs, and the OCS increases; (3) the membranous form (slight activation) characterized by pseudomyelinic structures; (4) the saccular stage (moderate activation) showing an ameboid PLT shape and saccular–tubular reorganizations

of the OCS and the onset of degranulation; (5) the pseudopodical stage (strong activation) showing numerous cell projections containing prominent microfibrils present mainly in the periphery of PLTs. In this stage, the degranulation is already completed; (6) the hyaline stage refers to the end of the activation process, where shadows of granules and "obscure fibrillar" structures are visible.

Former concepts describing the dynamics of the MTC have to be revised. It can be demonstrated that after exposure of PLTs to agonists, the MTC remains intact. In the course of activation, the MTC becomes constricted into tight rings around centrally concentrated granules. During the process of irreversible aggregation and clot retraction, the MTC disintegrate, and groups of individual polymers appear in pseudopods or are oriented in the long axis of the PLTs. It has been shown that the MTC consists of a single polymer that is wound in 8–12 coils in the periphery of the cytoplasm [63, 64]. However, three-dimensional cryoelectron tomographic reconstructions of individually traced microtubules showed that some circumferential microtubules end at OCS invaginations. They are sometimes incomplete and occasionally reveal interconnections [65]. The release reaction implicates the fusion of granules with the OCS where they disintegrate. The fusion event is not easily followed by TEM. In our image (Figure 6), such a fusion could be demonstrated using rapid cryofixation followed by cryosubstitution.

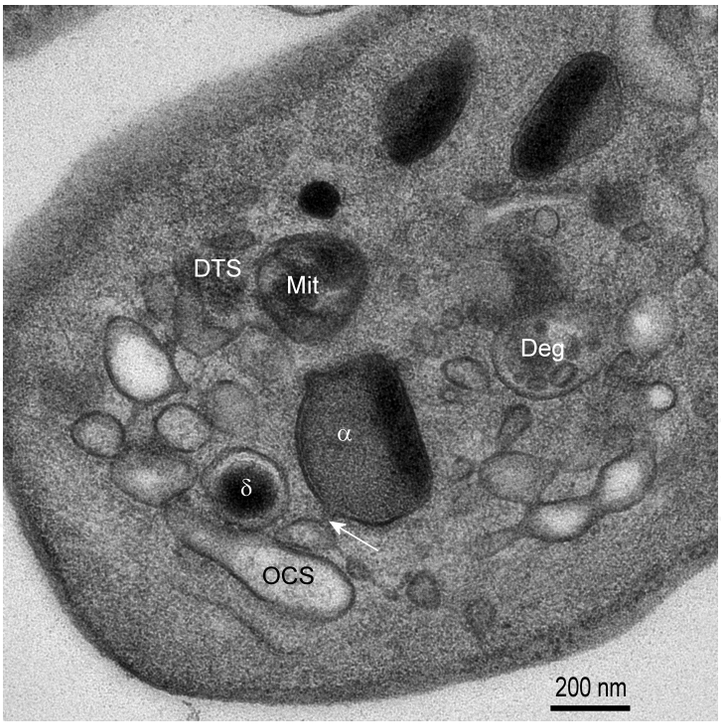

Figure 6. PLT showing the delivery of α-granules content into the OCS. Preparation by high-pressure fixation and cryosubstitution into Epon. PLTs from an apheresis PC were sucked into cellulose tubes that were closed at both ends and subjected to high-pressure fixation. 70 nm ultrathin sections were viewed under a Tecnai 20 electron microscope, and digital images were acquired using an Eagle 4k bottom-mount camera (FEI Co.). The connection between an α-granule and the OCS is indicated by the arrow. Abbreviations as in Figure 2.

http://dx.doi.org/10.5772/60673

2.5. Platelet Microparticles (PMP)

Among other cells such as endothelial and immune cells, PLTs are able to form PMPs which play a pivotal role in immunology and vascular biology. These particles are thought to be of significant clinical relevance as they can bind to and interact with macrophages, neutrophil granulocytes, and endothelial cells [102, 103]. They were first described already in 1967 by Wolf et al. [104]. PLTs form two types of PMPs differing in size and molecular composition [105]. One type is relatively large with diameters ranging from 100 nm to 1 μm expressing $GP\alpha_{IIb}$-β_3, GPIbα, and CD62P and exhibiting the apoptosis marker phosphatidylserine at the plasma membrane. Therefore, they can be identified via binding of annexin V. The second type of PMPs, corresponding to ectosomes, is smaller than 100 nm and expresses CD63, a membrane-spanning protein, present on α-granules which is translocated to the PM during PLT activation [106, 107]. They interact poorly only weakly with annexin V, do not bind prothrombin and factor X, and therefore have probably no coagulation function [108]. Among others [109], these authors separated PMPs by differential centrifugation in order to remove red and white blood cells as well as PLT followed by ultracentrifugation. PMPs, present in PLT-free plasma, were absorbed to filmed EM grids and investigated in the TEM after negative staining [108, 109]. Other groups investigated pellets of PMP, embedded in epoxy resin [106, 107].

In our own studies, pelleted PMPs were trapped in alginate beads, classically embedded, thin sectioned, and viewed under a TEM (Figure 7).

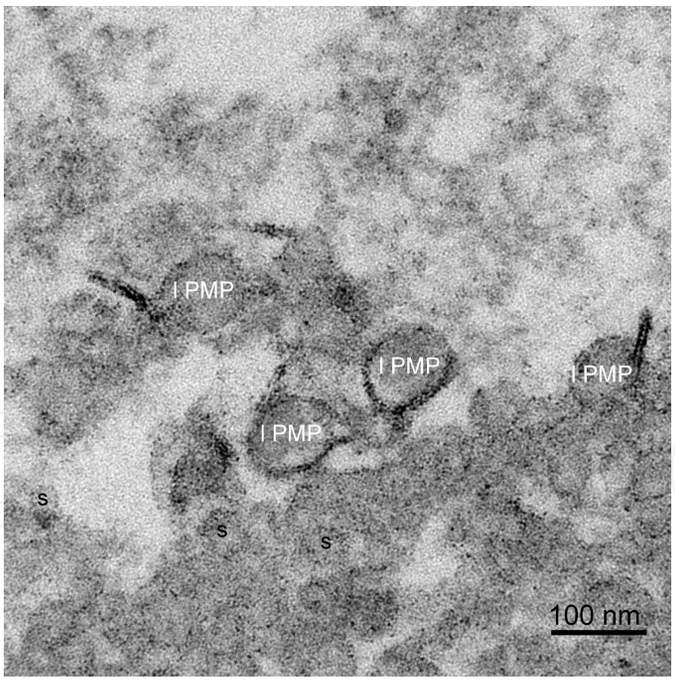

Figure 7. PMPs embedded in alginate beads. Larger PMPs (l PMP) ≥ 100 nm and aggregated small PMPs could be distinguished. Chemical fixation, dehydration, and embedding in Epon. 70 nm ultrathin sections were viewed under a Tecnai 20 electron microscope, and digital images were acquired using an Eagle 4k bottom-mount camera (FEI Co.).

We were able to visualize the formation of PMPs on glass-adherent PLTs. TEM images showed that small vesicular elements developed in a protrusion of a PLT. A close association of these

tightly packed vesicles with the DTS could be observed. The formation of such a multivesicular sphere and its delivery from the PLT is shown after using electron tomographic reconstruction. We suggest that microvesicles are delivered from this harboring ball-like structure (Figure 8).

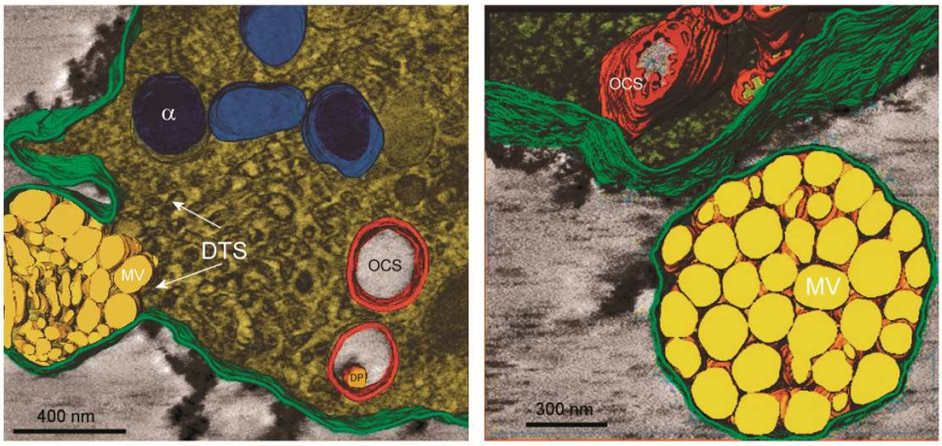

Figure 8. Formation of PLT protrusions containing microvesicles, demonstrated in an electron tomographic 3D model. Figure 8a shows the formation of a sac, filled with microvesicles; Figure 8b its delivery. Chemical fixation, dehydration, and embedding in Epon. 70 nm ultrathin sections were viewed under a Tecnai 20 electron microscope, and digital images were acquired using an Eagle 4k bottom-mount camera (FEI Co.).

3. Ultrastructural evaluation of PLT activation using TEM is suitable to monitor PC production

3.1. Production of PC

PCs can be produced by apheresis machines or by pooling of buffy coats obtained from whole blood donations. There is a long-lasting and long-winded discussion about the advantages and disadvantages of both methods [110]. To produce PC by apheresis, blood from a healthy donor is collected and subjected to centrifugation in an apheresis device, where blood cells are separated according to their density. Blood cells, with exception of PLTs, are reinfused. The technical features of the most common apheresis machines differ significantly with respect to stress on PLTs such as centrifugation and shear forces and their duration. In addition, the degree of contamination with residual leukocytes depends on the particular machine. Sometimes, apheresis machines produce higher leukocyte rates and have to be filtered using a leukocyte depletion filter to avoid side effects and complications in the recipient.

Buffy-coat-derived PCs are produced by two-step centrifugation method. Whole blood is collected into triple bags containing CPD in the primary bag and centrifuged at 4000 × *g* for 10 min at 22 °C within 12 h. Red blood cells and plasma are separated from the buffy coat fraction and transferred into satellite containers by using an automated separator. Subsequently, buffy coats from four different donors and one bag containing either 300 ml plasma from one of the four donors or PLT additive solution are connected by using a sterile connection device and

http://dx.doi.org/10.5772/60673

were pooled in one container. Subsequently a 1 l polyolefin bag and a leukocyte reduction filter are connected. This pool is then centrifuged at 500 × *g* for 8 min at 22 °C. The supernatant is squeezed out immediately into the storage bag by means of a plasma extractor [111].

PCs are stored in gas-permeable plastic bags for 5–7 days. In our experience, all manufacturing processes induce a slight PLT activation which might be also reversible. With lasting storage time, dead PLTs caused by necrosis but also by apoptosis [112–114] occur. Early stages of apoptosis can be detected by binding of annexin V to the exposed phosphatidylserine of the plasma membrane. At the ultrastructural level, this can be visualized by binding of a complex, consisting of annexin V, a specific antibody, and gold-labeled protein A to the PLT surface [115]. In late stages of apoptosis and necrosis, the PLT fine structure is then characterized by the loss in the integrity of membranes and by extraction of the cytoplasm that contains remnants of granules and cytoskeleton.

In a recent publication [111], we described a method to evaluate the alterations of PLTs at a single cell level. The method can be carried out easily in routine EM laboratories. A pre-fixation of PCs was done by mixing 9 ml PC with 1 ml of a 10 % buffered formaldehyde solution (BD CellFIX™, Becton Dickinson, Vienna, Austria) in order to avoid shape changes of PLT by the subsequent preparation steps. Immediately after pre-fixation, the samples were centrifuged at 800 x g for 10 min at 22 °C. After discarding the supernatant, the pellet was fixed with 10 ml of 2.5 % glutaraldehyde (Fluka, Vienna, Austria) in cacodylate buffer, pH 7.2, for 90 min at 4 °C. After fixation, the PLTs were washed twice by centrifugation at 800 x g for 10 min at 4 °C, transferred to 2 ml Eppendorf vials (Eppendorf AG, Hamburg, Germany), pelleted again, and fixed with 1 % O_sO_4 (Fluka) for 90 min, dehydrated in a graded series of ethanol (50, 70, 90, 96 and 100 %) and embedded in Epon (Serva, Heidelberg, Germany). Sections (70–80 nm) of Epon-embedded cells were cut with an UltraCut UCT ultramicrotome (Leica Inc., Vienna, Austria), transferred to copper grids, and routinely stained with uranyl acetate and lead citrate. The sections were viewed either under an EM900 transmission electron microscope (Carl Zeiss, Oberkochen, Germany), equipped with a 1k wide angle slow-scan CCD camera, allowing distortion-free images for photomontages (Tröndle, Munich, Germany) at 50 kV or under a Tecnai 20 transmission electron microscope (FEI Co., Eindhoven, The Netherlands) and a 1k slow-scan bottom-mount CCD camera (MSC 794, Gatan Inc., Pleasanton, CA, USA) at 80 kV. The panorama views consisting of eight single digital images at a magnification of 3000x providing a resolution of about 3700 x 1800 pixels.

- Score 0: unchanged discoid form showing the peripheral MTC in the equatorial plane (Figure 9a) or in the cross section (Figure 9 b)
- Score 1: formation of filopodia and dilatation of the OCS (Figure 9c)
- Score 2: pronounced shape alterations, centralization of the MTC and proceeding degranulation (white arrows; Figure 9d)
- Score 3: degeneration with alteration of the plasma membrane and necrosis (Figure 9e)
- In addition, also the formation of aggregates can be visualized (Figure 9f). Note that PLTs in the center of the aggregate are degranulated. All PLTs are connected among each other by interdigitating filopodia

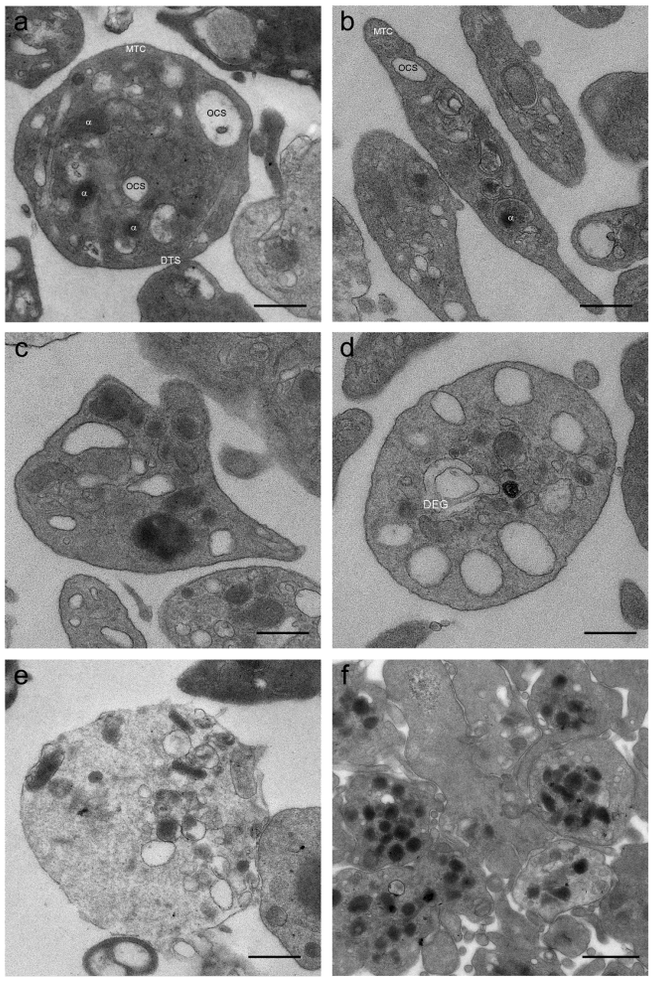

Figure 9. Stages of activation and degeneration of PLTs. The morphological evaluation of PLTs in TEM panorama views is based on a score classification of the individual PLT according to the following criteria:

Size bars: 500 nm in Figure 1a–e, 1 μm in Figure 1f. The samples were routinely prepared by chemical fixation, dehydration, and embedding in Epon, and 70 nm ultrathin sections were viewed under a Tecnai 20 (FEI Co.) at 80 KV acceleration voltage. Digital images were acquired using an Eagle 4k bottom-mount camera (FEI Co.).

PLTs representing a particular score value were counted using the analySIS® morphometry software (Soft Imaging System, Münster, Germany). The score values can be used for statistics comparing different processing methods using parameter-free rank tests.

The advantage of our score classification consists in the registration of alterations and different activation stages of PLT caused by the manipulations during production of PCs. It can distinguish between slight and advanced PLT activation. In addition, the presence of PLT aggregates is included in the evaluation. Nevertheless, one has to ignore PLTs that are only marginally sectioned, since in that case no appropriate evaluation is possible. The assembled images of the photomontages allow further zooming and a detailed analysis of subcellular features. The MTC and its centralization during PLT activation are only visible in equatorial

sections or in some cross sections. Early changes occur as strong dilatation of the OCS and formation of surface projections, while strongly activated PLTs show distinct signs of degranulation and frequently a budding of microparticles and ectosomes.

3.2. Examples on how EM can and has been applied for quality control of PC

EM can be used to examine PLT morphology in relation to different preparation and storage methods. Integrity as well as activation stages can be immediately monitored at single cell level. Further functional aspects can be investigated with automatized analytic systems such as flow cytometry, aggregometry turbometry, etc. The impact of the contribution of EM has already been pointed out by White and Krumwiede [116]. In this paper, the authors summarize the morphological features of PLTs and organelles such as MTC, α-granules, and the dense bodies in PLTs of healthy donors and patients suffering from the Hermansky–Pudlak syndrome and storage pool deficiency disorders as well as giant PLT diseases such as the white and the gray PLT syndrome. Another publication [117] describes the ultrastructural evaluation of PC function after intermittent-flow centrifugation apheresis collected from donors by combined platelet-leukapheresis with hydroxyethyl starch or by plateletpheresis without starch. The authors found that the PLT morphology was almost unchanged with the exception of glycogen granules being absent in PLTs isolated in presence of hydroxyethyl starch. They concluded that the starch did not significantly alter PLT morphology and PLT aggregation.

Forced by the occurrence of bovine spongiform encephalopathies (BSE), caused by prion infections in the United Kingdom and other countries in the 1990s of the last century, a better surveillance of blood donations and methods for the production of blood components has been introduced in most European countries [118]. In the course of these improvements, leucodepletion or better leukoreduction methods have been introduced as a new standard in blood banking. Even if it is unlikely that prions can be removed by leukoreduction, this procedure is able to prevent many side effects caused by unwanted cytokine release during storage. In this context some publications deal with the quality of PLTs after removal of white blood cells (WBCs). Using EM, no significant PLT alterations were found in surface modified polyester filters [119], in the filtration system (PL100) [120], as well as by using of the Sepacell PL system [121]. Similar results were obtained from prestorage WBC reduction filters designed for leukocyte depletion during the preparation of the pool PC from platelet-rich buffy coats [122]. Interestingly, in filters of WBC-depleted red blood cell concentrates, granulocyte depletion occurred also by indirect adhesion to activated and spread PLTs [123, 124].

Most of the authors, using EM to investigate PLT vitality, refer to the influence of storage conditions on the morphological appearance of PLTs [12, 68, 125–130]. Lactate accumulation may cause a pH fall in PC leading to a reduction of organelles and a progredient destruction of cell membranes [12, 126]. Storage of buffy-coat-derived PCs can be affected by the presence of residual WBCs [68] or due to additive solutions, partially replacing plasma. These solutions provoke increasing PLT activation and increasing chemokine release during storage [127]. Elias et al. described that a good maintenance of PLT ultrastructure could be achieved by adding a stable synthetic prostacyclin analogue (Iloprost) to the PC [128]. The chemical composition of storage bags can modify the adhesion of mononuclear cells to the plastic

substrate of the PLT storage bag and the release of cytokines. Bags composed of the polyolefin polymer induce a higher release of IL-1β, TNF-α, IL-6, and IL-8 compared to the single-donor apheresis polyvinyl chloride polymer platelet bags with the tri-(2-ethylhexyl) trimellitate (TEHTM) plasticizer. A similar study was carried out using polyvinyl chloride containers plasticized with tri(2-ethylhexyl) trimellitate (PL 1240 plastic) [129]. Even using the most advanced storage conditions, the quality of PLTs in PCs decreases significantly with storage time [127]. For this effect, the high storage temperature of 20 °C as well as a progressive loss of nutrients in the storage plasma or in the platelet additive solution as well as the accumulation of toxic metabolites can be taken into consideration. In our experience, the PLT activation is only slightly enhanced during storage time, while the percentage of necrotic PLTs increases significantly. In this respect, usually PCs are stored not longer than 5 days.

Ahnadi et al. [130] measured the ex vivo (basal) and in vitro (thrombin-induced) PLT activation in sodium citrate, ethylenediaminetetraacetic acid (EDTA), and citrate-theophylline-adenosine-dipyridamol (CTAD) in whole blood specimens. TEM studies verified shape modifications and simultaneous retention of granules at early post-venipuncture time periods in CTAD specimens.

Transfusion of washed PLTs is recommended for patients with history of allergic reactions. This procedure, commonly performed using neutral, calcium-free Ringer's acetate (NRA) can be performed before (prewash) or after storage of PC. Comparing the procedures, Kelley et al. [131] could not find any fine structural alterations even when the postwash procedure was carried out only after 6–7 days of storage. In addition, it could be demonstrated that the chemical structure of storage bags may induce cytokine release leading to alteration of PLT shape as demonstrated via SEM [132].

Some publications refer to the quality of chilled, frozen, or even lyophilized PLT. It has been demonstrated that long-term storage of fixed and lyophilized platelets that retain hemostatic properties after rehydration showed a rather normal ultrastructure [133]. Another option to increase the storage time is the cryopreservation of human PLTs. It has been shown that controlled-rate freezing procedure in combination with lower (6 %) Dimethylsulfoxide (DMSO) concentration resulted in less damage from freezing and higher recovered function of PLTs as revealed by light and electron microscopic parameters [134]. In contrast, Böck et al. observed clear signs of beginning cell necrosis after thawing and resuspension in autologous plasma [135].

An interesting field for EM investigations is the quality control of PC after pathogen inactivation and storage of pathogen-inactivated PCs. Advantages and controversies about this approach including the different techniques have been summarized in [136, 137]. Ultrastructural investigations are not available on this subject so far.

3.3. Interaction of PLTs with bacteria

PCs are stored at room temperature to avoid aggregation and injury of the plasma membrane. Therefore, problems of bacterial contamination and proliferation are increased. An estimation for bacterial contamination in the United States indicates that 1:1000–1:3000 of PCs leads to

http://dx.doi.org/10.5772/60673

severe life threatening complications in 1 out of 6 patients [138]. In contaminated PCs, the following kinds of bacteria could be detected: *Clostridium perfringens*, *Enterobacter cloacae*, *Escherichia coli*, *Flavobacterium* spp., *Klebsiella oxytoca*, *Propionibacterium acnes*, *Salmonella choleraesuis*, *Salmonella enterica* serotype enteritidis, *Salmonella enterica* serotype Heidelberg, *Serratia marcescens*, *Staphylococcus aureus*, *methicillin-resistant Staphylococcus aureus* (MRSA), *Staphylococcus carnosus*, *Staphylococcus epidermidis*, *Staphylococcus lugdunensis*, *Staphylococcus* spp. coagulase negative, *Streptococcus pneumoniae*, *Streptococcus pyogenes*, *Streptococcus viridans*, *Yersinia enterocolitica* serotype O:3. Bacterial contaminations can be caused by failures in blood drawing (mainly by insufficient disinfection of donor's skin), by leak plastic tubes, or the donor carries bacteria in his/her blood without clinical symptoms.

There exist different opinions about the ability of PLTs to kill bacteria. Even in some cases, PLTs exhibit adverse reactions for the host by transporting bacteria from the site of infection to another place in the circulation where they adhere and cause injury [139]. Nevertheless, as outlined in this review, PLTs are equipped with cell surface receptors reacting directly or indirectly with counter receptors and molecules at the bacterial wall. Among these PLT receptors, the fibrinogen receptor GPIIb/IIIa, the von Willebrand factor receptor GPIbα, the Fc receptor FcγRIIα, complement receptors, and toll-like receptors TLRs (belonging to the innate immune receptors) are functional. Indirect binding is mediated by fibrinogen, von Willebrand factor, complement, and IgG. PLTs can also produce bactericide agents such as β-lysins and PLT microbicidal proteins (PMPs) which do not induce lesions on the bacterial wall but interact with neutrophil granulocytes and lymphocytes, thrombin-induced PMPs (tPMPs), and their derivatives termed thrombocidins and kinocidins representing a subset of PMPs being classical chemokines that have direct microbicidal activity. They possess dual chemokine and microbicidal effector functions [140]. The host defense against bacteria induces an activated metabolic status, the change from discoid to ameboid shape with expression of receptors interacting with injured or infected tissues, the generation of oxygen radicals, as well as the extension of pseudopodia interacting with microbial pathogens. These changes are managed by the cytoskeleton which facilitates granule mobilization and degradation leading to the release of granule contents including host defense peptides.

In our own experiments, using electron tomography, we could impressively show that bacteria such *Escherichia coli* and *Streptococcus epidermidis* could cause their adhesion (Figure 10a), aggregation (Figure 10b), and engulfment (Figure 10a,c,d). Engulfment of bacteria is achieved by uptake into the OCS where they can be subsequently sequestered. The separation of parts of the OCS from the surrounding milieu was verified by the surface-coat-binding of the electron-dense dye ruthenium red. In sequestered areas of the OCS, both the membrane of the OCS and the bacterial wall remain unstained (Figure 10c), while in parts of the OCS that are in continuity with the environment, a distinct decoration of both structures could be found (Figure 10d). Preliminary studies with the pH-sensitive fluorescent dye pHrodo showed a decrease of pH in PLTs after engulfment of bacteria. In addition, killing of living bacteria could be demonstrated by fluorescence microscopy using the LIVE/DEAD® fixable dead cell stain kit (Life Technologies, Vienna, Austria).

There are different views concerning the phagocytic capacity of PLTs, one favoring the view of covercytes [141], others supporting the idea of phagocytosis. In this respect, Li et al. [142]

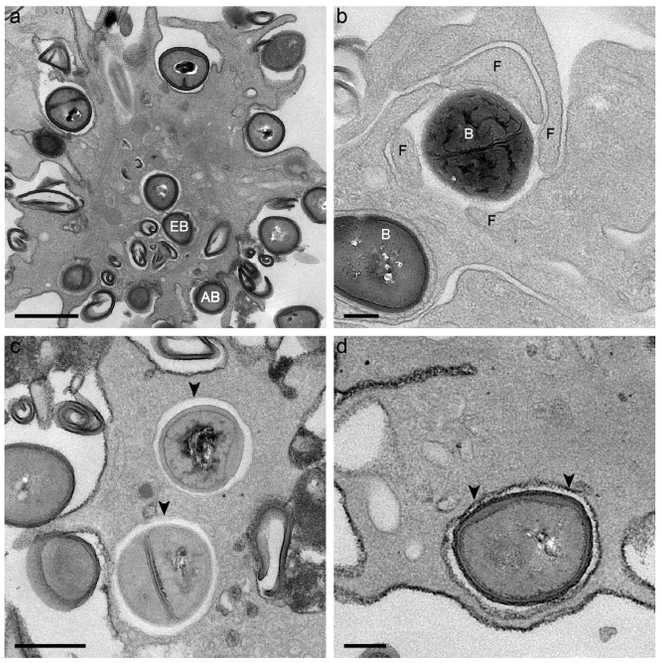

Figure 10. Adherent PLTs were stained with ruthenium red as tracer in order to show whether engulfed bacteria (*Staphylococcus epidermidis*) are still in contact with the extracellular milieu or separated from it. Figure 10a shows adhesion (AB) and engulfment of bacteria (EB). Figure 10b demonstrates the ability of PLTs to form aggregates by interdigitations of filopodia (F) in which bacteria (B) are sequestered. Figure 10c shows completely engulfed bacteria whereby both the membrane of the OCS (arrowheads) and the bacterial wall remain unstained. In contrast to this image, Figure 10d shows both parts decorated with ruthenium red, indicating that there exists still a communication with the surrounding milieu. Ultrathin sections were viewed under a Tecnai 20 electron microscope, and digital images were acquired using an Eagle 4k bottom-mount camera (FEI Co.).

reported the engulfment and phagocytosis of *Porphyromonas gingivalis* by ruthenium red staining. Using enzyme EM methods, as early as 1976, it could be demonstrated that phagocytosis of latex particles by PLTs leads to the formation of acid phosphatase-positive vesicles and to their killing and degradation [143].

In many countries, pathogen inactivation methods by cross linking of nucleic acids are used routinely (for reviews, see [144, 145]). There is much emphasis that transfusion-mediated infections can be avoided by these techniques. Nevertheless, several aspects concerning the function and recovery of pathogen-inactivated PCs in the recipient are still a matter of discussion.

4. Conclusion

PLTs are very dynamic cell fragments that display functions, widely exceeding those of blood coagulation [146]. Electron microscopy, implicating new techniques such as correlative microscopy, and the various variants of cryotechniques, combined with electron tomography, allow insights at high resolution, which cannot be achieved with other methods.

http://dx.doi.org/10.5772/60673

We would like to emphasize that EM analyses of PCs significantly supplement the routinely used quality assessment methods monitoring different manufacturing procedures. Methodical refinements, improving the preparation protocols of EM specimens, such as a wide range of cryomethods, stabilizing the samples close to the living state, together with electron tomography, 3D-reconstruction and modeling visualize structural details and dynamic processes at high resolution [99, 147, 148]. Thus new in vitro and in vivo tests of PLT function in transfused PCs can be efficiently controlled at the EM level. The technique is particularly helpful in the case a new apheresis system is introduced in a blood bank. EM evaluation of PLT qualities can significantly supplement the results obtained from commonly used laboratory methods.

Abbreviations

EM: electron microscopy; MK: megakaryocyte; PC: platelet concentrate; PLT: platelet, thrombocyte; PMPs: platelet membrane microparticles; PM: platelet membrane; TEM: transmission electron microscopy; OCS: open canalicular system; DTS: dense tubular system; DMS: demarcation membrane system; MTC: microtubular coil

Acknowledgements

The authors gratefully acknowledge the provision of apheresis PCs by Mrs. Renate Renz (Blood Donation Center of the Austrian Red Cross for Vienna, Lower Austria, and Burgenland), the skillful technical assistance of Mrs. Ivanna Federenko, Mrs. Beatrix Mallinger, and Mrs. Regina Wegscheider, and Mr. Ulrich Kaindl and Mr. Thomas Nardelli for their valuable help with the artwork and the 3D modeling (Center for Anatomy and Cell Biology, Department of Cell Biology and Ultrastructure Research, Medical University of Vienna).

Author details

Josef Neumüller[1], Adolf Ellinger[2] and Thomas Wagner[3*]

*Address all correspondence to: thomas.wagner@medunigraz.at

1 Blood Donation Center of the Austrian Red Cross for Vienna, Lower Austria, and Burgenland, Vienna, Austria

2 Medical University of Vienna, Center for Anatomy and Cell Biology, Department of Cell Biology and Ultrastructure Research, Vienna, Austria

3 Department of Blood Group Serology and Transfusion Medicine, Medical University of Graz, Graz, Austria

References

[1] Rebulla P. Revisitation of the clinical indications for the transfusion of platelet concentrates. Rev Clin Exp Hematol. 2001; 5(3): 288–310.

[2] Salama A, Kiesewetter H, Kalus U, Movassaghi K, Meyer O. Massive platelet transfusion is a rapidly effective emergency treatment in patients with refractory autoimmune thrombocytopenia. Thromb Haemost. 2008; 100(5): 762–765.

[3] Ali SF. Platelet activation of platelet concentrates derived from buffy coat and apheresis methods. Transfus Apher Sci. 2011; 44(1): 11–13.

[4] Altuntas F, Sari I, Kocyigit I, Kaynar L, Hacioglu S, Ozturk A, Oztekin M, Solmaz M, Eser B, Cetin M, Unal A. Comparison of plateletpheresis on the fenwal amicus and fresenius Com.Tec cell separators. Transfus Med Hemother. 2008; 35(5): 368–373.

[5] Bueno JL, Barea L, Garcia F, Castro E. A comparison of PLT collections from two apheresis devices. Transfusion. 2004; 44(1): 119–124.

[6] Burgstaler EA, Winters JL, Pineda AA. Paired comparison of Gambro Trima Accel versus Baxter Amicus single-needle plateletpheresis. Transfusion. 2004; 44(11): 1612–1620.

[7] Fontana S, Mordasini L, Keller P, Taleghani BM. Prospective, paired crossover comparison of multiple, single-needle plateletpheresis procedures with the Amicus and Trima Accel cell separators. Transfusion. 2006; 46(11): 2004–2010.

[8] Jilma-Stohlawetz P, Eichelberger B, Horvath M, Jilma B, Panzer S. In vitro platelet function of platelet concentrates prepared using three different apheresis devices determined by impedance and optical aggregometry. Transfusion. 2009; 49(8): 1564–1568.

[9] Perseghin P, Mascaretti L, Riva M, Sciorelli G. Comparison of plateletpheresis concentrates produced with Spectra LRS version 5.1 and LRS Turbo version 7.0 cell separators. Transfusion. 2000; 40(7): 789–793.

[10] Perseghin P, Mascaretti L, Speranza T, Belotti D, Baldini V, Dassi M, Riva M, Pogliani EM, Sciorelli G. Platelet activation during plasma-reduced multicomponent PLT collection: a comparison between COBE Trima and Spectra LRS turbo cell separators. Transfusion. 2004; 44(1): 125–130.

[11] Picker SM, Radojska SM, Gathof BS. Prospective comparison of high-dose plateletpheresis with the latest apheresis systems on the same donors. Transfusion. 2006; 46(9): 1601–1608.

[12] Ringwald J, Zingsem J, Zimmermann R, Strasser E, Antoon M, Eckstein R. First comparison of productivity and citrate donor load between the Trima version 4 (dual-

stage filler) and the Trima Accel (single-stage filler) in the same donors. Vox Sang. 2003; 85(4): 267–275.

[13] Seghatchian J, Krailadsiri P. The quality of MCS+ version C2 double dose platelet concentrate with leucodepletion through a continuous filtration process. Transfus Apher Sci. 2002; 26(1): 37–41.

[14] Zingsem J, Glaser A, Zimmermann R, Weisbach V, Kalb R, Ruf A, Eckstein R. Paired comparison of apheresis platelet function after storage in two containers. J Clin Apher. 2001; 16(1): 10–14.

[15] Zingsem J, Strasser E, Ringwald J, Zimmermann R, Weisbach V, Eckstein R. Evaluation of a new apheresis system for the collection of leukoreduced single-donor platelets. Transfusion. 2007; 47(6): 987–994.

[16] Picker SM. In-vitro assessment of platelet function. Transfus Apher Sci. 2011; 44(3): 305–319.

[17] Panzer S, Jilma P. Methods for testing platelet function for transfusion medicine. Vox Sang. 2011; 101(1): 1–9.

[18] Cognasse F, Hamzeh-Cognasse H, Lafarge S, Acquart S, Chavarin P, Courbil R, Fabrigli P, Garraud O. Donor platelets stored for at least 3 days can elicit activation marker expression by the recipient's blood mononuclear cells: an in vitro study. Transfusion. 2009; 49(1): 91–98.

[19] Spiess BD. Transfusion of blood products affects outcome in cardiac surgery. Semin Cardiothorac Vasc Anesth. 2004; 8(4): 267–281.

[20] Simak J, Gelderman MP. Cell membrane microparticles in blood and blood products: potentially pathogenic agents and diagnostic markers. Transfus Med Rev. 2006; 20(1): 1–26.

[21] Gilstad CW. Anaphylactic transfusion reactions. Curr Opin Hematol. 2003; 10(6): 419–423.

[22] White JG. The dense bodies of human platelets. Origin of serotonin storage particles from platelet granules. Am J Pathol. 1968; 53(5): 791–808.

[23] White JG. The submembrane filaments of blood platelets. Am J Pathol. 1969; 56(2): 267–277.

[24] White JG. Interaction of membrane systems in blood platelets. Am J Pathol. 1972; 66(2): 295–312.

[25] White JG. Identification of platelet secretion in the electron microscope. Ser Haematol. 1973; 6(3): 429–459.

[26] White JG. Morphological studies of platelets and platelet reactions. Vox Sang. 1981; 40(Suppl 1): 8–17.

[27] White JG. Cytoskeletal changes in aging platelets. Prog Clin Biol Res. 1985; 195: 49–77.

[28] White JG. An overview of platelet structural physiology. Scanning Microsc. 1987; 1(4): 1677–1700.

[29] White JG. Ultrastructural analysis of platelet contractile apparatus. Methods Enzymol. 1992; 215: 109–127.

[30] White JG. Platelet secretory granules and associated proteins. Lab Invest. 1993; 68(5): 497–498.

[31] White JG. Platelet secretory process. Blood. 1999; 93(7): 2422–2425.

[32] White JG. Electron microscopy methods for studying platelet structure and function. Methods Mol Biol. 2004; 272: 47–63.

[33] White JG. Electron opaque structures in human platelets: which are or are not dense bodies? Platelets. 2008; 19(6): 455–466.

[34] White JG, Escolar G. The blood platelet open canalicular system: a two-way street. Eur J Cell Biol. 1991; 56(2): 233–242.

[35] White JG, Estensen RD. Degranulation of discoid platelets. Am J Pathol. 1972; 68(2): 289–302.

[36] White JG, Gerrard JM. Ultrastructural features of abnormal blood platelets. A review. Am J Pathol. 1976; 83(3): 589–632.

[37] White JG, Gerrard JM. Platelet ultrastructure in relation to platelet function. Prog Clin Biol Res. 1978; 28: 5–23.

[38] White JG, Gerrard JM. Interaction of microtubules and microfilaments in platelet contractile physiology. Methods Achiev Exp Pathol. 1979; 9: 1–39.

[39] White JG, Krivit W. The ultrastructural localization and release of platelet lipids. Blood. 1966; 27(2): 167–186.

[40] White JG, Sauk JJ. Microtubule coils in spread blood platelets. Blood. 1984; 64(2) 470–478.

[41] White JG. Ultrastructural defects in congenital disorders of platelet function. Ann N Y Acad Sci. 1972; 201: 205–33.

[42] White JG. Platelet microtubules and giant granules in the Chediak-Higashi syndrome. Am J Med Technol. 1978; 44(4): 273–278.

[43] White JG. Ultrastructural studies of the gray platelet syndrome. Am J Pathol. 1979; 95(2): 445–462.

[44] White JG. Membrane defects in inherited disorders of platelet function. Am J Pediatr Hematol Oncol. 1982; 4(1): 83–94.

[45] White JG. Platelet granule disorders. Crit Rev Oncol Hematol. 1986; 4(4): 337–377.

[46] White JG. Use of the electron microscope for diagnosis of platelet disorders. Semin Thromb Hemost. 1998; 24(2): 163–168.

[47] White JG. Golgi complexes in hypogranular platelet syndromes. Platelets. 2005; 16(1): 51–60.

[48] White JG, de Alarcon PA. Platelet spherocytosis: a new bleeding disorder. Am J Hematol. 2002; 70(2): 158–166.

[49] White JG, Gerrard JM. The ultrastructure of defective human platelets. Mol Cell Biochem. 1978; 21(2): 109–128.

[50] Bessis M, Breton-Gorius J. Microtubules and fibrils in spread-out platelets. Nouv Rev Fr Hematol. 1965; 5(4): 657–662.

[51] Bessis M, Dreyfus B, Breton-Gorius J, Sultan C. Electron microscopic study of 11 cases of refractory anemias with multiple enzymopathies. Nouv Rev Fr Hematol. 1969; 9(1): 87–104.

[52] Berry S, Dawicki DD, Agarwal KC, Steiner M. The role of microtubules in platelet secretory release. Biochim Biophys Acta. 1989; 1012(1): 46–56.

[53] Escolar G, Sauk J, Bravo ML, Krumwiede M, White JG. Immunogold staining of microtubules in resting and activated platelets. Am J Hematol. 1987; 24(2): 177–188.

[54] Italiano JE, Jr., Bergmeier W, Tiwari S, Falet H, Hartwig JH, Hoffmeister KM, Andre P, Wagner DD, Shivdasani RA. Mechanisms and implications of platelet discoid shape. Blood. 2003; 101(12): 4789–4796.

[55] Lewis JC. Cytoskeleton in platelet function. Cell Muscle Motil. 1984; 5: 341–377.

[56] Radley JM, Hartshorn MA. Megakaryocyte fragments and the microtubule coil. Blood Cells. 1987; 12(3): 603–614.

[57] Spangenberg P. The cytoskeleton of platelets. Acta Histochem Suppl. 1990; 39: 385–395.

[58] White JG. Tubular elements in platelet granules. Blood. 1968; 32(1): 148–156.

[59] Xu Z, Afzelius BA. The substructure of marginal bundles in human blood platelets. J Ultrastruct Mol Struct Res. 1988; 99(3): 244–253.

[60] Xu Z, Afzelius BA. Early changes in the substructure of the marginal bundle in human blood platelets responding to adenosine diphosphate. J Ultrastruct Mol Struct Res. 1988; 99(3): 254–260.

[61] Canizares C, Vivar N, Tenesaca S. Analysis of the ultrastructure of the platelets during the process of aggregation, with emphasis in the cytoskeleton and membranous changes. Microsc Electron Biol Celular. 1988; 12(1): 1–15.

[62] White JG. Arrangements of actin filaments in the cytoskeleton of human platelets. Am J Pathol. 1984; 117(2): 207–217.

[63] Escolar G, White JG. The platelet open canalicular system: a final common pathway. Blood Cells. 1991; 17(3): 467–485; discussion 86–95.

[64] Escolar G, Leistikow E, White JG. The fate of the open canalicular system in surface and suspension-activated platelets. Blood. 1989; 74(6): 1983–1988.

[65] White JG. Platelets are covercytes, not phagocytes: uptake of bacteria involves channels of the open canalicular system. Platelets. 2005; 16(2): 121–131.

[66] Canizares C, Vivar N, Herdoiza M. Role of the microtubular system in platelet aggregation. Braz J Med Biol Res. 1994; 27: 1533–1551.

[67] Clawson CC, Rao GH, White JG. Platelet interaction with bacteria. IV. Stimulation of the release reaction. Am J Pathol. 1975; 81(2): 411–420.

[68] Daimon T, Gotoh Y, Kawai K, Uchida K. Ultrastructural distribution of peroxidase in thrombocytes of mammals and submammals. Histochemistry. 1985; 82(4): 345–350.

[69] Ebbeling L, Robertson C, McNicol A, Gerrard JM. Rapid ultrastructural changes in the dense tubular system following platelet activation. Blood. 1992; 80(3): 718–723.

[70] Gerrard JM, White JG, Peterson DA. The platelet dense tubular system: its relationship to prostaglandin synthesis and calcium flux. Thromb Haemost. 1978; 40(2): 224–231.

[71] Gerrard JM, White JG, Rao GH, Townsend D. Localization of platelet prostaglandin production in the platelet dense tubular system. Am J Pathol. 1976; 83(2): 283–298.

[72] Rendu F, Brohard-Bohn B. The platelet release reaction: granules' constituents, secretion and functions. Platelets. 2001; 12(5): 261–273.

[73] Saussy DL, Jr., Mais DE, Baron DA, Pepkowitz SH, Halushka PV. Subcellular localization of a thromboxane A2/prostaglandin H2 receptor antagonist binding site in human platelets. Biochem Pharmacol. 1988; 37(4): 647–654.

[74] van Nispen Tot Pannerden HE, van Dijk SM, Du V, Heijnen HF. Platelet protein disulfide isomerase is localized in the dense tubular system and does not become surface expressed after activation. Blood. 2009; 114(21): 4738–4740.

[75] White JG, Conard WJ. The fine structure of freeze-fractured blood platelets. Am J Pathol. 1973; 70(1): 45–56.

[76] Zhao B, Dierichs R, Liu JF, Zhu ZM, Berkes P, Frye S. Influence of low density lipoproteins on cytosolic free Ca^{2+} concentration and dense tubular system in human platelets. Thromb Res. 1993; 72(1): 33–37.

[77] Behnke O. Degrading and non-degrading pathways in fluid-phase (non-adsorptive) endocytosis in human blood platelets. J Submicrosc Cytol Pathol. 1992; 24(2): 169–178.

[78] Bentfeld-Barker ME, Bainton DF. Identification of primary lysosomes in human megakaryocytes and platelets. Blood. 1982; 59(3): 472–481.

[79] Stenberg PE, McEver RP, Shuman MA, Jacques YV, Bainton DF. A platelet alpha-granule membrane protein (GMP-140) is expressed on the plasma membrane after activation. J Cell Biol. 1985; 101(3): 880–886.

[80] Lewis JC, Hantgan RR, Stevenson SC, Thornburg T, Kieffer N, Guichard J, Breton-Gorius J. Fibrinogen and glycoprotein lib/Illa localization during platelet adhesion. Localization to the granulomere and at sites of platelet interaction. Am J Pathol. 1990; 136(1): 239–252.

[81] Machlus KR, Italiano JE Jr. The incredible journey: from megakaryocyte development to platelet formation. J Cell Biol. 2013; 201(6): 785–796.

[82] Bartley TD, Bogenberger J, Hunt P, Li YS, Lu HS, Martin F, Chang MS, Samal B, Nichol JL, Swift S, et al. Identification and cloning of a megakaryocyte growth and development factor that is a ligand for the cytokine receptor Mpl Cell. 1994; 77(1): 1117–1124.

[83] de Sauvage FJ, Hass PE, Spencer SD, Malloy BE, Gurney AL, Spencer SA, Darbonne WC, Henzel WJ, Wong SC, Kuang WJ, et al. Stimulation of megakaryocytopoiesis and thrombopoiesis by the c-Mpl ligand. Nature. 1994; 369(6481): 533–538.

[84] Kaushansky K. The mpl ligand: molecular and cellular biology of the critical regulator of megakaryocyte development. Stem Cells. 1994; 12(Suppl. 1): 91–96, discussion 96–97.

[85] Zimmet J, Ravid K. Polyploidy: occurrence in nature, mechanisms, and significance for the megakaryocyte-platelet system. Exp. Hematol. 2000; 28(1): 3–16.

[86] Eckly A, Heijnen H, Pertuy F, Geerts W, Proamer F, Rinckel JY, Léon C, Lanza F, Gachet C. Biogenesis of the demarcation membrane system (DMS) in megakaryocytes. Blood. 2014; 123(6): 921–930.

[87] Patel-Hett S, Wang H, Begonja AJ, Thon JN, Alden EC, Wandersee NJ, An X, Mohandas N, Hartwig JH, Italiano JE Jr. The spectrin based membrane skeleton stabilizes mouse megakaryocyte membrane systems and is essential for proplatelet and platelet formation. Blood. 2011; 118(6): 1641–1652.

[88] Thon JN, Montalvo A, Patel-Hett S, Devine MT, Richardson JL, Ehrlicher A, Larson MK, Hoffmeister K, Hartwig JH, Italiano JE Jr. Cytoskeletal mechanics of proplatelet maturation and platelet release. J Cell Biol. 2010; 191(4): 861–874.

[89] Thon JN, Macleod H, Begonja AJ, Zhu J, Lee KC, Mogilner A, Hartwig JH, Italiano JE Jr. Microtubule and cortical forces determine platelet size during vascular platelet production. Nat Commun. 2012; 3: 852.

[90] Schachtner H, Calaminus SD, Sinclair A, Monypenny J, Blundell MP, Leon C, Holyoake TL, Thrasher AJ, Michie AM, Vukovic M, Gachet C, Jones GE, Thomas SG, Watson SP, Machesky LM. Megakaryocytes assemble podosomes that degrade matrix and protrude through basement membrane. Blood. 2013; 121(13): 2542–2552.

[91] Meddens MB, van den Dries K, Cambi A. Podosomes revealed by advanced bioimaging: what did we learn? Eur J Cell Biol. 2014; 93(10–12): 380–387.

[92] Gavazzi I, Nermut M, Marchisio PCV. Ultrastructure and gold-immunolabelling of cell-substratum adhesions (podosomes) in RSV-transformed BHK cells. J Cell Sci. 1989; 94(Pt 1): 85–99.

[93] Nitsch L, Gionti E, Cancedda R, Marchisio PC. The podosomes of Rous sarcoma virus transformed chondrocytes show a peculiar ultrastructural organization. Cell Biol Int Rep. 1989; 13(11): 919–926.

[94] Tarone G, Cirillo D, Giancotti FG, Comoglio PM, Marchisio PC. Rous sarcoma virus-transformed fibroblasts adhere primarily at discrete protrusions of the ventral membrane called podosomes. Exp Cell Res. 1985; 159(1): 141–157.

[95] Carman CV, Sage PT, Sciuto TE, de la Fuente MA, Geha RS, Ochs HD, Dvorak HF, Dvorak AM, Springer TA. Transcellular diapedesis is initiated by invasive podosomes. Immunity. 2007; 26(6): 784–797.

[96] Cougoule C, Van Goethem E, Le Cabec V, Lafouresse F, Dupré L, Mehraj V, Mège J-L, Lastrucci C, Maridonneau-Parini I. Blood leukocytes and macrophages of various phenotypes have distinct abilities to form podosomes and to migrate in 3D environments. Eur J Cell Biol. 2012; 91(11–12): 938–949.

[97] Gawden-Bone C, Zhou Z, King E, Prescott A, Watts C, Lucocq J. Dendritic cell podosomes are protrusive and invade the extracellular matrix using metalloproteinase MMP-14. J Cell Sci. 2010; 123(Pt 9): 1427–1437.

[98] Van Goethem E, Guiet R, Balor S, Charrière GM, Poincloux R, Labrousse A,Maridonneau-Parini I, Le Cabec V. Macrophage podosomes go 3D. Eur J Cell Biol. 2013; 90(2–3): 224–236.

[99] van Nispen tot Pannerden H, de Haas F, Geerts W, Posthuma G, van Dijk S, Heijnen HF. the platelet interior revisited: electron tomography reveals tubular alpha-granule subtypes. Blood. 2010; 116: 1147–1156.

[100] Rivera J, Lozano ML, Navarro-Núñez L, Vicente V. Platelet receptors and signaling in the dynamics of thrombus formation. Haematologica. 2009; 94(5): 700–711.

[101] Ren Q, Ye S, Whiteheart SW. The platelet release reaction: just when you thought platelet secretion was simple. Curr Opin Hematol. 2008; 15(5): 537–541.

[102] Thushara RM, Hemshekhar M, Basappa, Kemparaju K, Rangappa KS, Girish KS. Biologicals, platelet apoptosis and human diseases: an outlook. Crit Rev Oncol Hematol. 2014; pii: S 1040-8428 (14)00186-3.

[103] Burnouf T, Goubran HA, Chou ML, Devos D, Radosevic M. Platelet microparticles: detection and assessment of their paradoxical functional roles in disease and regenerative medicine. Blood Rev. 2014; 28(4): 155–166.

[104] Wolf P. The nature and significance of platelet products in human plasma. Br J Haematol. 1967; 13(3): 269–288.

[105] Heijnen HF, Schiel AE, Fijnheer R, Geuze HJ, Sixma JJ. Activated platelets release two types of membrane vesicles: microvesicles by surface shedding and exosomes derived from exocytosis of multivesicular bodies and alpha-granules. Blood. 1999; 94(11): 3791–3799.

[106] Gambim MH, do Carmo Ade O, Marti L, Veríssimo-Filho S, Lopes LR, Janiszewski M. Platelet-derived exosomes induce endothelial cell apoptosis through peroxynitrite generation: experimental evidence for a novel mechanism of septic vascular dysfunction. Crit Care. 2007; 11(5): 1–12.

[107] Hughes M, Hayward CP, Warkentin TE, Horsewood P, Chorneyko KA, Kelton JG. Morphological analysis of microparticle generation in heparin-induced thrombocytopenia. Blood. 2000; 96(1): 188–194.

[108] Sadallah S, Eken C, Martin PJ, Schifferli JA. Microparticles (ectosomes) shed by stored human platelets downregulate macrophages and modify the development of dendritic cells. J Immunol. 2011; 186(11): 6543–6552.

[109] Aatonen MT, Öhman T, Nyman TA, Laitinen S, Grönholm M, Siljander PR. Isolation and characterization of platelet-derived extracellular vesicles. J Extracell Vesicles. 2014; 3: 24692.

[110] Schrezenmeier H, Seifried E. Buffy-coat-derived pooled platelet concentrates and apheresis platelet concentrates: which product type should be preferred? Vox Sang. 2010; 105(6): 783–791.

[111] Neumüller J, Meisslitzer-Ruppitsch C, Ellinger A, Pavelka M, Jungbauer C, Renz R, Leitner G, Wagner T. Monitoring of platelet activation in platelet concentrates using transmission electron microscopy. Transfus Med Hemother. 2013; 40(2): 101–107.

[112] Leytin V, Freedman J. Platelet apoptosis in stored platelet concentrates and other models. Transfus Apher Sci. 2003; 28(3): 285–295.

[113] Leytin V. Apoptosis in the anucleate platelet. Blood Rev. 2012; 26(2): 51–63.

[114] Ohto H, Nollet KE. Overview on platelet preservation: better controls over storage lesion. Transfus Apher Sci. 2011; 44(3): 321–325.

[115] Stuart MC, Bevers EM, Comfurius P, Zwaal RF, Reutelingsperger CP, Frederik PM. Ultrastructural detection of surface exposed phosphatidylserine on activated blood platelets. Thromb Haemost. 1995; 74(4): 1145–1151.

[116] White JG, Krumwiede M. Some contributions of electron microscopy to knowledge of human platelets. Thromb Haemost. 2007; 98(1): 69–72.

[117] Maguire LC, Henriksen RA, Strauss RG, Stein MN, Goedken MM, Echternacht B, Koepke JA, Thompson JS. Function and morphology of platelets produced for transfusion by intermittent-flow centrifugation plateletpheresis or combined platelet-leukapheresis. Transfusion. 1981; 21(1): 118–123.

[118] Foster PR. Prions and blood products. Ann Med. 2000; 32(7): 501–513.

[119] Böck M, Heim MU, Weindler R, Bilas A, Greither L, Salat C, Mempel W. White cell depletion of single-donor platelet preparations by a new adsorption filter. Transfusion. 1991; 31(4): 333–334.

[120] Böck M, Himmelsbach S, Gudden A, Greither L, Mempel W. Preparation of leukocyte-depleted thrombocyte concentrate: in-vitro testing of a new filtration system (PL 100). Infusionstherapie. 1991; 18(1): 30–32.

[121] Böck M, Salat C, Greither L, Heim MU, Weindler R, Bilas A, Mempel W. Production of leukocyte-poor thrombocyte concentrates: results with a new kind of filter system. Beitr Infusionsther. 1990; 26: 103–105.

[122] Christensen LD, Dickmeiss E. In vitro evaluation of a new filter for leucocyte depletion of platelet concentrate during component preparation. Vox Sang. 1994; 67(3): 267–271.

[123] Steneker I, Prins HK, Florie M, Loos JA, Biewenga J. Mechanisms of white cell reduction in red cell concentrates by filtration: the effect of the cellular composition of the red cell concentrates. Transfusion. 1993; 33(1): 42–50.

[124] Steneker I, van Luyn MJ, van Wachem PB, Biewenga J. Electron microscopic examination of white cell reduction by four white cell-reduction filters. Transfusion. 1992; 32(5): 450–457.

[125] Böck M, Greither L, Gudden A, Diehm H, Heim MU, Mempel W. Storage of thrombocyte concentrates: ultrastructural and functional changes. Infusionstherapie. 1991; 18(3): 137–138, 141–142.

[126] Bertolini F, Porretti L, Lauri E, Rebulla P, Sirchia G. Role of lactate in platelet storage lesion. Vox Sang. 1993; 65(3): 194–198.

[127] Wagner T, Vetter A, Dimovic N, Guber SE, Helmberg W, Kroll W, Lanzer G, Mayr WR, Neumüller J. Ultrastructural changes and activation differences in platelet concentrates stored in plasma and additive solution. Transfusion. 2002; 42(6): 719–727.

[128] Elias M, Heethuis A, Weggemans M, Bom V, Blom N, McShine RL, Halie MR, Smit Sibinga CT. Stabilization of standard platelet concentrates and minimization of the platelet storage lesion by a prostacyclin analogue. Ann Hematol. 1992; 64(6): 292–298.

[129] Grode G, Miripol J, Garber J, Barber T, Buchholz DH. Extended storage of platelets in a new plastic container. I. Biochemical and morphologic changes. Transfusion. 1985; 25(3): 204–208.

[130] Ahnadi CE, Sabrinah Chapman E, Lepine M, Okrongly D, Pujol-Moix N, Hernandez A, Boughrassa F, Grant AM. Assessment of platelet activation in several different anticoagulants by the Advia 120 hematology system, fluorescence flow cytometry, and electron microscopy. Thromb Haemost. 2003; 90(5): 940–948.

[131] Kelley WE, Edelman BB, Drachenberg CB, Hess JR. Washing platelets in neutral, calcium-free, Ringer's acetate. Transfusion. 2009; 49(9): 1917–1923.

[132] ElKattan I, Anderson J, Yun JK, Colton E, Yomtovian R. Correlation of cytokine elaboration with mononuclear cell adhesion to platelet storage bag plastic polymers: a pilot study. Clin Diagn Lab Immunol. 1999; 6(4): 509–513.

[133] Read MS, Reddick RL, Bode AP, Bellinger DA, Nichols TC, Taylor K, Smith SV, McMahon DK, Griggs TR, Brinkhous KM. Preservation of hemostatic and structural properties of rehydrated lyophilized platelets: potential for long-term storage of dried platelets for transfusion. Proc Natl Acad Sci USA. 1995; 92(2): 397–401.

[134] Balint B, Vucetic D, Trajkovic-Lakic Z, Petakov M, Bugarski D, Brajuskovic G, Taseski J. Quantitative, functional, morphological and ultrastructural recovery of platelets as predictor for cryopreservation. Haematologia (Budap) 2002; 32(4): 363–375.

[135] Böck M, Greither L, Heim MU. Morphologic and functional changes in thrombocytes after deep freezing with DMSO. Infusionsther Transfusionsmed. 1996; 23(2): 76–79.

[136] Lindholm PF, Annen K, Ramsey G. Approaches to minimize infection risk in blood banking and transfusion practice. Infect Disord Drug Targets. 2011; 11(1): 45–56.

[137] Marwaha N, Sharma RR. Consensus and controversies in platelet transfusion. Transfus Apher Sci. 2009; 41(2): 127–133.

[138] Burns KH, Werchs JB. Bacterial contamination of platelet units: a case report and literature survey with review of upcoming American association of blood banks requirements. Arch Pathol Lab Med. 2004; 128(3): 279–281.

[139] Cox D, Kerrigan SW, Watson SP. Platelets and the innate immune system: mechanisms of bacterial-induced platelet activation. J Thromb Haemost. 2011; 9(6): 1097–1107.

[140] Yeaman MR. Platelets in defense against bacterial pathogens. Cell Mol Life Sci. 2010; 67(4): 525–544.

[141] White JG. Platelets are covercytes, not phagocytes: uptake of bacteria involves channels of the open canalicular system. Platelets. 2005 16(2): 121–131.

[142] Li X, Iwai T, Nakamura H, Inoue Y, Chen Y, Umeda M, Suzuki H. An ultrastructural study of porphyromonas gingivalis-induced platelet aggregation. Thromb Res. 2008; 122(6): 810–819.

[143] Lewis JC, Maldonado JE, Mann KG. Phagocytosis in human platelets: localization of acid phosphatase-positive phagosomes following latex uptake. Blood. 1976; 47(5): 833–840.

[144] Kaiser-Guignard J, Canellini G, Lion N, Abonnenc M, Osselaer JC, Tissot JD. The clinical and biological impact of new pathogen inactivation technologies on platelet concentrates. Blood Rev. 2014; 28(6): 235–241.

[145] Lozano M, Cid J. Analysis of reasons for not implementing pathogen inactivation for platelet concentrates. Transfus Clin Biol. 2013; 20(2): 158–164.

[146] Leslie M. Cell biology. Beyond clotting: the powers of platelets. Science. 2010; 328(5978): 562–564.

[147] Ellinger A, Vetterlein M, Weiss C, Meisslitzer-Ruppitsch C, Neumüller J, Pavelka M. High-pressure freezing combined with in vivo-DAB-cytochemistry: a novel approach for studies of endocytic compartments. J Struct Biol. 2011; 169(3): 286–293.

[148] Meisslitzer-Ruppitsch C, Röhrl C, Ranftler C, Neumüller J, Vetterlein M, Ellinger A, Pavelka M. The ceramide-enriched trans-Golgi compartments reorganize together with other parts of the Golgi apparatus in response to ATP-depletion. Histochem Cell Biol. 2011; 135(2): 159–171.